Thermodynamic Considerations of Triblock Copolymers with a Random Middle Block

John M. Zielinski†

Department of Chemical Engineering, The Pennsylvania State University, University Park, Pennsylvania 16802

Richard J. Spontak*

Miami Valley Laboratories, Procter & Gamble Company, Cincinnati, Ohio 45239

Received October 21, 1991; Revised Manuscript Received July 20, 1992

ABSTRACT: Experimental studies have shown that the thermomechanical properties of microphase-separated AB diblock copolymers are strongly dependent on the fraction of material residing within the interphase region. The degree of interfacial mixing is determined principally from the chemical dissimilarity between the blocks and can be controlled by judicious choice of A and B monomers. Another method of tailoring the interphase is by chemical insertion of a random A/B block between the pure A and B end blocks. If the end blocks of such an A(A/B)B triblock copolymer are pure and the "domain-boundary-mixing" effect dominates, only the interphase region is enlarged by this addition. A sufficiently long A/B block is postulated here to self-assemble into its own microphase, thereby producing a morphology consisting of three distinct microphases under proper conditions. A thermodynamic model based on confined-chain statistics is proposed to predict the strong-segregation phase behavior and microstructural dimensions of such a system. Predictions provided in this work address these issues as explicit functions of block composition, molecular composition, and molecular weight. Other molecular design considerations, e.g., compositional tapering of the A/B block, are also discussed.

Introduction

Since interphase zones reflect the intimate molecular contact between phases in composite materials, an understanding of these regions is prerequisite for the efficient design of multiphasic polymer alloys with specific thermomechanical properties. Consequently, considerable attention has continually been drawn to detailed characterization of the interphase in microphase-separated block copolymers.[1-3] Quantification of the size of this region has been possible with scattering techniques such as small-angle X-ray scattering (SAXS),[4-6] small-angle neutron scattering (SANS),[7-9] and, most recently, neutron reflectivity (NR).[10-12] Results from these studies have revealed that the interphase thickness in strongly-segregated poly(styrene-*b*-diene) diblock copolymers, for instance, is approximately 1.2–1.5 nm, which is in quantitative agreement with predictions obtained from theoretical models[13-15] devoted to the strong-segregation limit (SSL). This interphase, shown schematically in Figure 1a as λ_{AB}, is often relatively narrow in comparison to the characteristic lengths (L_A and L_B) of the microdomains.

Small-angle scattering studies,[16-20] along with dynamic mechanical testing,[21] have also proven very useful in demonstrating that these biphasic materials can, under proper conditions, undergo a weak first-order phase transition referred to as either the microphase-separation transition (MST) or the order–disorder transition (ODT). According to the theory proposed by Leibler[22] for the weak-segregation limit (WSL), an AB diblock copolymer possessing a lamellar morphology (50/50 composition) undergoes its ODT when $\chi_{AB}(T)N \approx 10.5$, where $\chi_{AB}(T)$ is the temperature-dependent Flory–Huggins interaction parameter and N is the degree of polymerization of the molecule. A correlation proposed[23] for $\chi_{SI}(T)$ of poly-

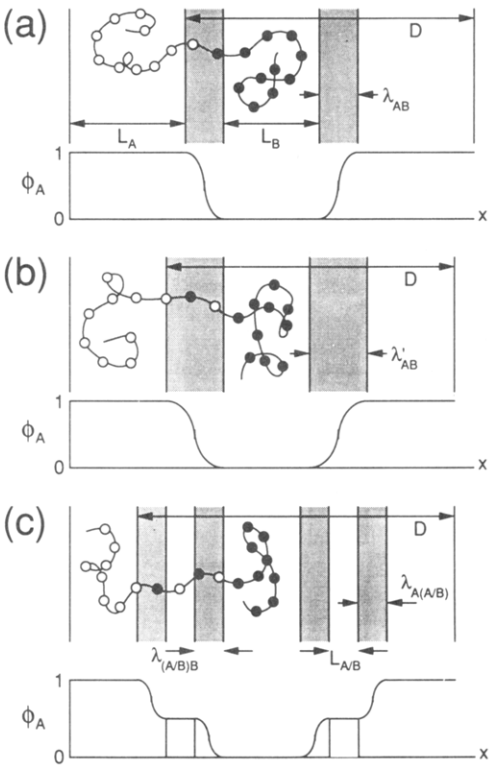

Figure 1. Schematic illustrations of the three lamellar morphologies that a microphase-separated A(A/B)B block copolymer is postulated to exhibit. In (a) there is no middle A/B block, and the system corresponds to an ideal diblock copolymer. If a relatively short A/B block is chemically inserted between the pure A and B end blocks and if the "domain-boundary-mixing" effect[24] dominates, the resultant morphology (b) appears similar to that of the diblock with an enlarged interphase (λ'_{AB}). If the A, A/B, and B blocks are all sufficiently long, a three-microphase morphology (c) is expected, in which case the middle microdomain consists of two interphases ($\lambda_{A(A/B)}$ and $\lambda_{(A/B)B}$) and a region ($L_{A/B}$) of constant mixed composition. The variation of composition (ϕ_A) with position (x) in microdomain space is also provided for each case.

* To whom correspondence should be addressed at the Department of Materials Science and Engineering, North Carolina State University, Raleigh, NC 27695.

† Present address: Performance Chemicals Technology, Air Products and Chemicals Inc., Allentown, PA 18195.

0024-9297/92/2225-5957$03.00/0

(styrene–isoprene) diblock (SI) copolymers is given by $\chi_{SI} \approx 71.4T^{-1} - 0.0857$ and can be used to estimate critical values of N at the ODT. These range from about 100 at the glass transition temperature of polystyrene (T_g = 100 °C) to 270 at 300 °C for SI copolymers (the corresponding equivalent molecular weights are approximately 8000 and 22 000, respectively). Neglecting the effect of critical fluctuations and the dependence of T_g on the length of the styrene block, this simple analysis reveals that SI copolymers within only a relatively small range of chain lengths are capable of undergoing their ODT in the melt state before thermally decomposing.

In the event that molecules of higher molecular weight are required for particular applications, χ_{AB} can be modified through substitution of one or both monomer species. A decrease in the thermodynamic incompatibility between the blocks results in a lower ODT and enhances phase mixing by virtue of an enlarged interphase. The relationship between χ_{AB} and λ_{AB} is best exemplified by the *narrow interphase approximation*,[15] in which $\lambda_{AB} \sim \chi_{AB}^{-1/2}$. Another viable approach to tailoring the interfacial characteristics of a diblock copolymer is through modification of the block junction by chemical insertion of a random or tapered A/B block between the pure A and B end blocks. Copolymers of this type have been successfully synthesized and their morphological and mechanical properties investigated.[24-26]

One attempt[27] to model the equilibrium thermodynamics of A(A/B)B copolymers has employed confined-chain statistics originally developed[13,14] for AB diblock copolymers. If the A/B block is relatively short and is restricted to the interphase so that the "domain-boundary-mixing" effect[24] dominates, the added block acts only to extend the interphase without significantly affecting the molecular conformation (see Figure 1b). When the A/B block becomes sufficiently long, however, the copolymer is expected to exhibit a three-microphase morphology analogous to that found in ABC copolymers (see Figure 1c). In this case, the middle block possesses chemical characteristics intermediate to the two end blocks.

Since recent efforts[28] to model the microstructural dimensions of microphase-separated ABC block copolymers in the SSL with confined-chain statistics have been successful, a similar and consistent formalism is applied in this work to the A(A/B)B molecular design. In addition to predicting system energetics and microstructural parameters as functions of molecular and block composition and molecular weight, an objective of the present work is to identify, at least semiquantitatively, the boundaries of the SSL.

Thermodynamic Theory

The present model assumes that the equilibrium morphology of a block copolymer can be accurately described by a single copolymer chain confined within a particular geometry in microdomain space. In this work, only the lamellar morphology is considered, for which the solution of the diffusion equation (needed to generate chain statistics) is exact. No provisions are made in this model to account for changes in morphology, which may become energetically favored under some conditions considered here.

A block copolymer is presumed to seek a state of equilibrium upon microphase separation, which is interpreted to mean that the difference in the molar Gibbs free energy (Δg) between the microphase-separated and homogeneous states is minimized with respect to each region of the postulated morphology:

$$\partial \Delta g / \partial A_i = 0 \; (i = 1, 2, 3, ..., m) \tag{1}$$

Here, A_i is the length of the ith microdomain region and m is the number of regions to be considered in the minimization. In the A(A/B)B design, m = 5 since there are three distinct block cores (L_i, where i = A, A/B, or B, as in Figure 1c) and two unrelated interphases ($\lambda_{A(A/B)}$ and $\lambda_{(A/B)B}$). In general, $\lambda_{A(A/B)} \neq \lambda_{(A/B)B}$. The minimized Δg function can also be written in terms of its enthalpic (Δh) and entropic (Δs) contributions, i.e.

$$\Delta g_{min} = (\Delta h - T\Delta s)_{min} \tag{2}$$

where T is the value of the absolute temperature (held constant at 298 K throughout this work). Only conditions yielding negative Δg_{min} for monomolecular systems correspond to a microphase-separated morphology and are considered here. This requirement, therefore, constitutes the first boundary condition of this formalism, namely, $\Delta g_{min} \approx 0$. Microstructural dimensions are determined implicitly from Δh and Δs in eq 2 or explicitly from the values of A_i in eq 1.

The enthalpy (Δh) is separated into two parts, one corresponding to complete phase demixing ($\Delta h^{(1)}$) and the other to residual interphase mixing ($\Delta h^{(2)}$):

$$\Delta h = \Delta h^{(1)} + \Delta h^{(2)} \tag{3}$$

The first contribution ($\Delta h^{(1)}$) can be calculated for an A(A/B)B system by invoking the Flory[29] equation

$$\Delta h^{(1)} = -v[\Delta\delta_{A(A/B)}{}^2\Phi_A\Phi_{A/B} + \Delta\delta_{AB}{}^2\Phi_A\Phi_B + \Delta\delta_{(A/B)B}{}^2\Phi_{A/B}\Phi_B] \tag{4}$$

Here, v is the total molar volume, which assuming incompressibility is equal to $\sum_i v_i$ (i = A, B, and A/B). Each of these v_i is determined from w_iM/ρ_i, with w_i and ρ_i being the weight fraction and mass density, respectively, of block i and M the molecular weight of the system. The volume-fraction composition of each block in the copolymer molecule is denoted as Φ_i, and $\Delta\delta_{ij}{}^2$ is the square of the difference in solubility parameters (δ) between blocks i and j. Physical properties (e.g., δ and ρ) of the pure A and B blocks are derived from the parent homopolymers (polystyrene and polyisoprene, respectively, in this work).[28] However, property estimation of the random A/B block requires appropriate mixing rules. If $\omega_A{}^{(A/B)}$ is the average weight fraction of component A in the A/B block, then

$$\omega_B{}^{(A/B)} = 1 - \omega_A{}^{(A/B)} \tag{5a}$$

$$\frac{1}{\rho_{A/B}} = \frac{\omega_A{}^{(A/B)}}{\rho_A} + \frac{\omega_B{}^{(A/B)}}{\rho_B} \tag{5b}$$

$$\phi_A{}^{(A/B)} = \frac{\omega_A{}^{(A/B)}/\rho_A}{\omega_A{}^{(A/B)}/\rho_A + \omega_B{}^{(A/B)}/\rho_B} \tag{5c}$$

$$\phi_B{}^{(A/B)} = 1 - \phi_A{}^{(A/B)} \tag{5d}$$

$$\delta_{A/B} = \phi_A{}^{(A/B)}\delta_A + \phi_B{}^{(A/B)}\delta_B \tag{5e}[30]$$

Note that $\omega_i{}^{(j)}$ and $\phi_i{}^{(j)}$ refer throughout this work to the weight- and volume-fraction compositions, respectively,

of species i in block j and that, unless otherwise indicated, $\omega_A^{(A/B)}$ is spatially invariant.[31]

The expression for $\Delta h^{(2)}$, which accounts for the mixed interphase regions, is similar to that derived[28] for an ABC copolymer but accounts for a middle block of intermediate composition ($\phi_A^{(A/B)}$):

$$\Delta h^{(2)} = \frac{v}{8}\{f_{A(A/B)}\Delta\delta_{A(A/B)}^2[4(1+\phi_A^{(A/B)}) - 3(1+(\phi_A^{(A/B)})^2) + \tau_{A(A/B)}\pi^2(1-\phi_A^{(A/B)})^2] + f_{(A/B)B}\Delta\delta_{(A/B)B}^2[4\phi_A^{(A/B)} - (3-\tau_{(A/B)B}\pi^2)(\phi_A^{(A/B)})^2]\} \quad (6)$$

where f_{ij} is the volume fraction of material remaining mixed upon microphase separation and is equal to $2\lambda_{ij}/D$ in the lamellar morphology, λ_{ij} is the thickness of the interphase between microphases i and j, and D is the microdomain periodicity (shown in Figure 1c). Since microdomains A and B are not adjacent, no f_{AB} term arises. The normalized long-range interaction parameters in eq 6 (τ_{ij}) are equal to $t^2/6\lambda_{ij}^2$ (where t is the Debye length equal to approximately 0.6 nm in condensed matter[13]). An assumption implicitly made in eq 6 is that the interfacial composition profiles across $\lambda_{A(A/B)}$ and $\lambda_{(A/B)B}$ can be represented by the sinusoidal function used in previous studies.[28,32]

The entropic function (Δs) in eq 2 is sensitive to both architecture and morphology. It is also expressed here as the sum of two contributions: one relating to restriction of the block junction between blocks i and j to the ij interphase ($\Delta s^{(1)}$) and the other to confinement of block i to its appropriate region in microdomain space ($\Delta s^{(2)}$). The probability of finding a given block junction in any given ij interphase is the volume fraction of interfacial material (f_{ij}), and the corresponding expression for $\Delta s^{(1)}$ is

$$\Delta s^{(1)} = R(\ln f_{A(A/B)} + \ln f_{(A/B)B}) \quad (7)$$

where R is the gas constant. The second term ($\Delta s^{(2)}$) arises from confinement of block i to T_i (i = A, A/B, or B) in microdomain space, where T_i spans the ith core (L_i) plus the two adjacent interphases. Forcing a block to remain within a specific region results in a loss of entropy due to both restricted placement and elastic deformation. The entropic expressions associated with restricted placement utilize the probability function derived from solution of the diffusion equation in an infinite parallel-plate geometry (i.e., the lamellar morphology) and in the absence of a potential field.[13,14] The loss of entropy associated with block deformation is obtained from elasticity theory and, like the probability function, depends on the number of block free ends. Summation of all of these contributions yields

$$\frac{\Delta s^{(2)}}{R} = \ln\left[\frac{2}{\pi}\exp(\sigma_{A/B})\sin\left(\frac{\pi\beta_{A(A/B)}T_A}{2T_{A/B}}\right)\times\left(1-\cos\left(\frac{\pi\beta_{(A/B)B}T_B}{T_{A/B}}\right)\right)\right] - \frac{3}{2}(\alpha_{A/B}^2-1) + \sum_{i=A,B}\ln\left[\frac{4}{\pi}\exp(\sigma_i)\sin\left(\frac{\pi\beta_{i(A/B)}}{2}\right)\right] - \frac{3}{2}(\alpha_i^2-1-\ln\alpha_i^2) \quad (8)$$

Here, $\beta_{A(A/B)} \equiv \lambda_{A(A/B)}/T_A$ and $\beta_{(A/B)B} \equiv \lambda_{(A/B)B}/T_B$ are two of the three dimensionless parameters employed in the free-energy minimization. In addition, $\sigma_i = -\pi^2\langle r_i^2\rangle/(6T_i^2)$, where $\langle r_i^2\rangle$ is related to the block expansion coefficient (α_i) through

$$\alpha_i^2 \equiv \langle r_i^2\rangle/\langle r_i^2\rangle_0 \quad (9)$$

and $\langle r_i^2\rangle_0$ is obtained from $\langle r_i^2\rangle_0 = K_i^2 w_i M$. Values of the Kuhn segment lengths K_A and K_B are available in the literature, whereas $K_{A/B}$ is estimated from $K_{A/B} = \omega_A^{(A/B)}K_A + \omega_B^{(A/B)}K_B$.

Since a potential field is not imposed to guarantee uniform core density in confined-chain models (as it is in other theories[15]), the relationships developed by Meier[13] to minimize the deviation from incomplete volume filling are employed here. These relationships take the form of $T_i = (C\langle r_i^2\rangle)^{1/2}$, where the constant C is equal to 2.0 in the case of a block with one free end or 1.5 if both ends of the block are anchored. Thus

$$T_i = (2.0\langle r_i^2\rangle)^{1/2} \quad (i = \text{A or B}) \quad (10a)$$

$$T_{A/B} = (1.5\langle r_{A/B}^2\rangle)^{1/2} \quad (10b)$$

With the enthalpic and entropic terms now fully specified, Δg is minimized for any given set of molecular characteristics (w_i, M, and $\omega_i^{(A/B)}$) with respect to each distinct microdomain region. The number of minimization variables (m in eq 1) can, however, be reduced by noting that the number of block junctions must be conserved within any interphase. The result of this requirement dictates[13] that

$$\alpha_j^2 = \alpha_i^2\xi_{ij}^2(w_j/w_i) \quad (11)$$

where $\xi_{ij} = (\rho_i K_i/\rho_j K_j)$ and i and j denote adjacent microphases. This expression allows both $T_{A/B}$ and T_B to be coupled with T_A, thereby reducing the number of independent regions to three—T_A, $\lambda_{A(A/B)}$, and $\lambda_{(A/B)B}$—in the case of the A(A/B)B architecture. Since the two interphases are mutually exclusive, as in the case of an ABC copolymer, no further simplifications can be made. These three microstructural dimensions used in the free-energy minimization are made dimensionless through the definitions of $\beta_{A(A/B)}$ and $\beta_{(A/B)B}$ provided earlier and Γ, which is given by

$$\Gamma \equiv T_A^2/\langle r_A^2\rangle_0 \quad (12)$$

Values of $\beta_{A(A/B)}$, $\beta_{(A/B)B}$, and Γ are subsequently used to obtain microstructural dimensions in these A(A/B)B triblock copolymers at equilibrium when the following conditions are met:

$$\left(\frac{\partial\Delta g}{\partial\beta_{A(A/B)}}\right) = \left(\frac{\partial\Delta g}{\partial\beta_{(A/B)B}}\right) = \left(\frac{\partial\Delta g}{\partial\Gamma}\right) = 0 \quad (13)$$

All of the predictions obtained with this model must reflect microstructural dimensions which are physically realistic. Values of β_{ij}, where ij corresponds to either A(A/B) or (A/B)B, are therefore restricted to the following boundary conditions: (i) $\beta_{ij} = 0$, when an interphase becomes vanishingly small, and (ii) $\beta_{ij} = {}^1/_2$, when a microdomain core (L_i in Figure 1a,c) vanishes into an enlarged interphase (i.e., $L_i = 0$ and $T_i = 2\lambda_{ij}$). These constraints on β_{ij}, in addition to the one on Δg_{min}, constitute three of the boundary conditions employed to define the regime of model applicability. One final condition that must be met is $L_{A/B} > 0$. In the case when $L_{A/B} \le 0$, the three-microphase morphology postulated here is no longer considered valid.

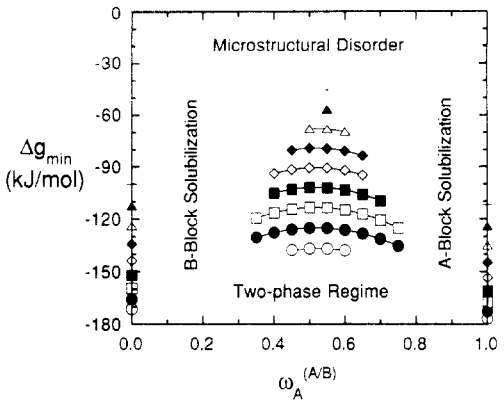

Figure 2. Predictions of Δg_{min} as a function of middle-block composition ($\omega_A^{(A/B)}$) for several molecular compositions ($w_{A/B}$): 0.20 (○), 0.25 (●), 0.30 (□), 0.35 (■), 0.40 (◇), 0.45 (◆), 0.50 (△), 0.55 (▲), and 0.60 (+). At large $w_{A/B}$, $\Delta g_{min} \to 0$, indicating microstructural disorder (or a transition to another morphology). The postulated three-microphase morphology degenerates into a two-microphase one at small $w_{A/B}$. If $\omega_A^{(A/B)}$ deviates sufficiently from 0.5, Δg_{min} decreases until an end block is preferentially solubilized. Predictions at $\omega_A^{(A/B)} = 0.0$ and $\omega_A^{(A/B)} = 1.0$ correspond to diblock copolymers with 30 and 70 wt % A, respectively. The molecular weight is held constant here at 2×10^5.

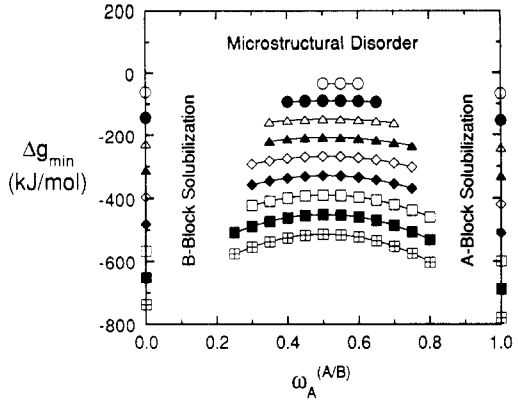

Figure 3. Predicted $\Delta g_{min}(\omega_A^{(A/B)})$ for different molecular weights (M), all expressed in 10^5: 1 (○), 2 (●), 3 (△), 4 (▲), 5 (◇), 6 (◆), 7 (□), 8 (■), and 9 (⊞). At low-M, $\Delta g_{min} \to 0$, one of the SSL boundary conditions. As M increases, Δg_{min} becomes increasingly more negative, suggesting an enhanced driving force toward microphase separation. Preferential end-block solubilization is once again predicted as $\omega_A^{(A/B)}$ deviates from 0.5. The end points at $\omega_A^{(A/B)}$ equal to zero and unity are analogous to those in Figure 2. In all of these predictions, $w_A = w_B = 0.3$ and $w_{A/B} = 0.4$.

Results and Discussion

An A(A/B)B block copolymer with a relatively large A/B fraction inherently possesses several adjustable molecular parameters, of which only block composition, molecular composition, and molecular weight are addressed explicitly here. In this work, we have selected combinations of molecular properties to illustrate key features of general interest. For instance, when the molecular composition (i.e., the weight fraction of the A/B middle block, $w_{A/B}$) is varied, the total molecular weight (M) is held constant at 2×10^5. When M is varied, the composition of the molecule is fixed at $w_A = w_B = 0.3$ and $w_{A/B} = 0.4$.

I. Range of Model Applicability. Before discussing predictions of microstructural dimensions obtained with the present formalism, the range of model applicability must be established. Recall that the constraints on Δg_{min}, β_{ij}, and $L_{A/B}$ listed earlier are presumed to constitute reasonable boundary conditions for the SSL. With these constraints in mind, predictions for free-energy minima as functions of both molecular and block composition ($w_{A/B}$ and $\omega_A^{(A/B)}$, respectively) are presented in Figure 2. In this figure, both $w_{A/B}$ and $\omega_A^{(A/B)}$ are incremented by 0.05. Below $w_{A/B} = 0.2$, model predictions are not given since $L_{A/B} \leq 0$, which implies that the copolymer exists as a two-microphase system with an enlarged interphase region (as in Figure 1b). Above this value of $w_{A/B}$, the copolymer is predicted to behave as a three-microphase system. As $w_{A/B}$ is increased further, Δg_{min} clearly becomes more positive until $\Delta g_{min} \geq 0$ and the model is again no longer applicable. While Figure 2 labels the regime at which $\Delta g_{min} \geq 0$ as "microstructurally disordered", recent evidence[33] suggests that a transition to a different morphology precedes thermodynamic disorder.

Figure 2 also illustrates that Δg_{min} reaches a maximum when the composition of the A/B block ($\omega_A^{(A/B)}$) is approximately 0.5 and decreases as $\omega_A^{(A/B)}$ deviates from the midpoint composition. As $\omega_A^{(A/B)}$ deviates from 0.5, the bulk weight-fraction composition of component A in the copolymer (W_A) also deviates from the midpoint composition according to

$$W_A = \omega_A^{(A)} w_A + \omega_A^{(A/B)} w_{A/B} + \omega_A^{(B)} w_B \qquad (14)$$

where $\omega_A^{(A)}$ and $\omega_A^{(B)}$ are taken here as unity and zero, respectively. (An analogous expression may be written for the bulk volume-fraction composition.) It must also be remembered that the A/B block in this instance possesses a random monomer sequence such that the average volume-fraction composition of the A/B block, $\phi_A^{(A/B)}$, is spatially invariant, as illustrated in Figure 1c. The imposition of a composition gradient across the A/B block, to produce a *tapered* block copolymer,[24,34-36] is discussed later. Another interesting feature regarding $\Delta g_{min}(\omega_A^{(A/B)})$ at constant $w_{A/B}$ in Figure 2 is that the model fails beyond certain values of $\omega_A^{(A/B)}$ due to violation of the boundary conditions on β_{ij}, implying that an end block is solubilized with the middle block. When $\omega_A^{(A/B)} \to 0$, the B block is solubilized, and when $\omega_A^{(A/B)} \to 1$, the A block is solubilized. This predicted behavior of *preferential end-block solubilization* suggests that *one* block pair (either A–A/B or A/B–B) may remain in the SSL while the other pair interacts in the WSL. Predictions for the cases when the middle block is either pure A or pure B (corresponding to asymmetric diblock copolymers) are also provided for comparison in Figure 2. It is certainly tempting to believe that Δg_{min} is a continuous function of $\omega_A^{(A/B)}$ from zero to unity, traversing the two end-block solubilization regimes, but no evidence currently exists to support this hypothesis.

In the predictions presented in Figure 3, the molecular composition is held constant at $w_{A/B} = 0.4$ and the total molecular weight (M) is varied from 10^5 to 9×10^5, in increments of 10^5. At sufficiently low M, $\Delta g_{min} \to 0$, in which case the model is no longer applicable. As M increases, Δg_{min} becomes increasingly more negative, indicating that the three-microphase system postulated here becomes more energetically favored. This observation may explain why this morphology has not yet been reported, since most of the A(A/B)B copolymers studied thus far have possessed values of M near 10^5.[24,25] Bühler and Gronski[26] have employed transmission electron microscopy (TEM) and dynamic mechanical testing in their investigations of several poly[styrene-*b*-(styrene-*ran*-isoprene)-*b*-isoprene] copolymers with higher molecular

weights (up to 193 000) but possessing <25 wt % of the isoprene end block. Their results indicate that such materials exhibit a dispersed spherical morphology when w_B is sufficiently large. It should be noted that, in their work, $w_{A/B}$ was increased in their copolymer series at the expense of decreasing w_B, which eventually led to an impure diblock copolymer possessing A and A/B blocks only. In this latter case, mixing occurs within the A/B microdomain core. (This topic is discussed further in the appendix.)

The behavior of Δg_{min} as a function of A/B block composition $\omega_A^{(A/B)}$ in Figure 3 is identical to that in Figure 2, with the exception that the range of $\omega_A^{(A/B)}$ over which the three-microphase system is predicted to exist increases with M. As M increases, however, two additional factors must be considered. The first is that entanglement effects will become increasingly more important and will eventually prevent the molecules from attaining thermodynamic equilibrium. The second issue is not as intuitive and pertains to the details of the middle A/B block. Recent theoretical efforts[31] have demonstrated that the monomer sequencing in a statistically random copolymer melt dictates whether the melt remains homogeneous or becomes mesomorphic. If sufficient driving force exists, A- or B-rich sequences along the random A/B block are expected to self-assemble into micelles. Rather than address the issue of monomer sequencing explicitly in the present work, we assume that the hypothetical middle A/B block remains completely homogeneous, even after microphase separation. Clearly, this is an oversimplification, but it permits us to treat A(A/B)B copolymers much in the same way as ternary ABC copolymers. The possibility of monomer self-assembly within the A/B microdomain should, however, be borne in mind.

While the SSL boundary conditions listed earlier provide a systematic method for ascertaining the range of model applicability, the absolute limits must be accepted with some caution. Estimates of the molecular characteristics corresponding to the WSL can be obtained from Leibler's theory[22] by treating these A(A/B)B copolymers as composites of two distinct diblock copolymers, each possessing $\chi_{i(A/B)}N \approx 10.5$ (i = A or B) at the WSL. The degree of polymerization (N) for each hypothetical diblock is determined directly from its molecular weight and composition, noting that these are *not* the same as those of the A(A/B)B triblock. For instance, M^* ($=w_iM + w_{A/B}M$) is the molecular weight of the i(A/B) diblock, and $w^*_{A/B}$ ($=w_{A/B}M/M^*$) is the renormalized weight fraction of the A/B block. Likewise, $\chi_{i(A/B)}$ is estimated from its relationship to $\Delta\delta_{i(A/B)}$,[30] which is an explicit function of block composition (see eq 5e). By assuming that these hypothetical diblocks are noninteracting (which becomes invalid at small $w_{A/B}$), the onset of the WSL is predicted to occur at $\omega_A^{(A/B)} \approx 0.22$ and $\omega_A^{(A/B)} \approx 0.82$ for all of the values of $w_{A/B}$ shown in Figure 2. These limits on $\omega_A^{(A/B)}$ are found to be more dependent on M (Figure 3), ranging from approximately 0.32 and 0.73 at $M = 10^5$ to 0.11 and 0.91 at $M = 9 \times 10^5$. If the assumptions made here accurately represent the conditions associated with the ODT, this analysis indicates that the predictions presented in Figures 2 and 3 reside within the SSL.

The most important concept established in this section is that a three-microphase morphology is thermodynamically favored in two-monomer A(A/B)B triblock copolymers under certain conditions of composition (both block and molecular) and chain length. The microstructural predictions provided throughout the remainder of this work are in accord with the boundary conditions discussed earlier and correspond to the regimes shown in both Figures 2 and 3.

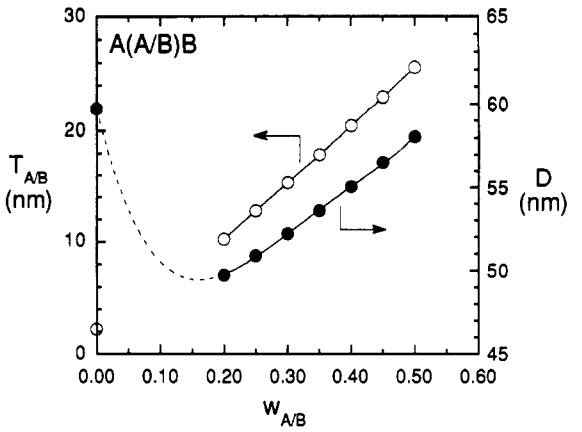

Figure 4. Dependence of the microdomain periodicity D (●) and mixed region $T_{A/B}$ (○) on molar composition, denoted here by $w_{A/B}$. Above $w_{A/B} = 0.2$, both D and $T_{A/B}$ increase with $w_{A/B}$. At $w_{A/B} = 0.0$, which corresponds to a diblock copolymer with no middle A/B block, D is greater than that for which $w_{A/B} > 0.2$. The dashed line (obtained by a fourth-degree polynomial fit of the predicted D and provided for illustrative purposes only) demonstrates that $D(w_{A/B})$ must possess a minimum within $0.0 < w_{A/B} < 0.2$. This feature implies that the length of the middle A/B block dictates both the degree of phase mixing and the onset of a three-microphase morphology. At $w_{A/B} = 0.0$, $T_{A/B}$ correctly reduces to the value of λ_{AB} in Figure 1a. The composition of the A/B block is held constant here at 0.5, and $M = 2 \times 10^5$.

II. Effect of Molecular Composition. The functional relationships of $D(w_{A/B})$ and $T_{A/B}(w_{A/B})$ obtained from the present model when $\omega_A^{(A/B)} = 0.5$ are shown in Figure 4. The periodicity D, illustrated in Figure 1c, is determined from

$$D = L_A + L_B + 2T_{A/B} \tag{15}$$

where

$$T_{A/B} = \lambda_{A(A/B)} + L_{A/B} + \lambda_{(A/B)B} \tag{16}$$

Here, $T_{A/B}$ constitutes the continuous region remaining mixed upon microphase separation. As is seen from Figure 4, both D and $T_{A/B}$ increase with the weight fraction of the middle block ($w_{A/B}$) in the three-microphase regime. However, when $w_{A/B} = 0$ (which corresponds to the ideal two-microphase system), D is greater than that predicted for any of the three-microphase systems in which $w_{A/B} > 0.2$. This observation implies that D reaches a minimum as a function of $w_{A/B}$ in the transition regime between two and three microphases. One plausible explanation for this trend is that insertion of a short A/B block mixes the system significantly, thereby reducing D. Substantial mixing continues as the A/B block is lengthened until the middle region becomes established as a separate microdomain, at which point the copolymer behaves as a pseudo three-component ABC system. Even though D is predicted to increase with $w_{A/B}$, the magnitude of D corresponding to three distinct microdomains at, say, $w_{A/B} = 0.5$ is comparable to that of the corresponding diblock, for which $w_{A/B} = 0$. The predicted $T_{A/B}$ at $w_{A/B} = 0$ correctly reduces to λ_{AB} in a two-microphase system (see Figure 1a).

III. Effect of Molecular Weight. Figure 3 illustrates that the three-microdomain system postulated here becomes more energetically favored at large M. In this section, we explore the effect of M on microstructural dimensions, in particular, $T_{A/B}$ and D. The functional relationship of $T_{A/B}(M)$ is plotted on double-logarithmic coordinates in Figure 5. A scaling relationship of the form $T_{A/B} \sim M^a$ is observed here and is useful in discerning the

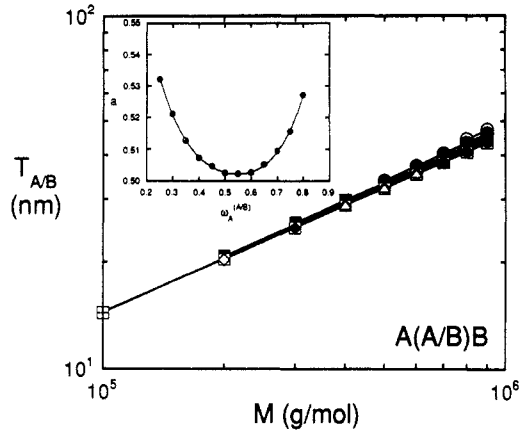

Figure 5. Plot of $T_{A/B}(M)$ revealing that $T_{A/B} \sim M^a$ over a wide variety of A/B block compositions: 0.25 (○), 0.30 (●), 0.35 (□), 0.40 (■), 0.45 (*), 0.50 (+), 0.55 (×), 0.60 (⊞), 0.65 (◇), 0.70 (♦), 0.75 (△), and 0.80 (▲). (Many of the predicted $T_{A/B}$ shown here coincide and are not readily seen in this figure.) In the inset, the values of the scaling exponent a are presented as a function of $\omega_A^{(A/B)}$ and indicate that $a \approx 0.51$. The predictions shown here employ $w_A = w_B = 0.3$ and $w_{A/B} = 0.4$.

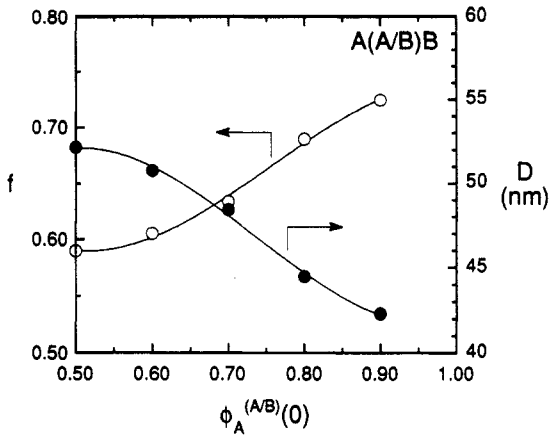

Figure 6. Predicted f (○) and D (●) as functions of $\phi_A^{(A/B)}(0)$. As the A/B block deviates from one that is spatially invariant to one that possesses a symmetric composition profile, D is predicted to decrease, while f is observed to increase substantially. These trends suggest that a tapered A/B middle block enhances solubilization of both end blocks.

conformation of the part of the copolymer chain residing within this region. Values of the scaling exponent a are shown as a function of $\omega_A^{(A/B)}$ in the inset and are found to lie within the range of 0.50–0.53. This observation implies that the part of the chain within $T_{A/B}$ appears to behave as an undeformed Gaussian coil. Recall, however, that $T_{A/B} = L_{A/B} + \lambda_{A(A/B)} + \lambda_{(A/B)B}$ (eq 16). Predictions for $L_{A/B}(M)$ reveal that the middle A/B block is actually stretched along the lamellar normal. The $T_{A/B}(M)$ relationship observed in Figure 5 reflects the average conformation of the A/B core *and* the two adjacent interphases, both of which are predicted to decrease with increasing M. The function $D(M)$ is not presented here but appears similar to that provided elsewhere[28] for ABC copolymers. It also exhibits a scaling relationship of the form $D \sim M^b$, where $b = 0.68 \pm 0.01$. This behavior indicates that the entire copolymer molecule is in an extended conformation, similar to the molecular conformations in conventional microphase-separated diblock and triblock copolymers.[4,37] While D is predicted to be proportional to M^b, the microdomain cores L_A, $L_{A/B}$, and L_B are not.

IV. Effect of Tapering. Throughout the preceding sections, the volume and weight fractions of A within the middle A/B block ($\phi_A^{(A/B)}$ and $\omega_A^{(A/B)}$, respectively) have been assumed to possess constant values across the mixed region $L_{A/B}$, thereby conforming to the compositional model shown schematically in Figure 1c. Due to poorly controlled polymerizations, for instance, it is more likely that the composition of the A/B block will vary continuously from being A-rich at one end to B-rich at the other. Copolymers possessing this type of middle block are said to be *tapered* and have been the subject of several studies.[24,34-36] Under these circumstances, $\phi_A^{(A/B)}$ is position dependent and is represented here by a symmetric sinusoidal function (the same employed to model the compositional variation across interphases). To facilitate model comparisons, we have chosen to fix the spatially-averaged volume fraction of component A ($\langle\phi_A^{(A/B)}\rangle$) at 0.5, which dictates that $\phi_A^{(A/B)}(1) = 1 - \phi_A^{(A/B)}(0)$, where the positions (0) and (1) refer to the A and B sides, respectively, of the A/B block. The composition profile used in the previous sections corresponds to the limiting case when $\phi_A^{(A/B)}(0) = \phi_A^{(A/B)}(1)$.

Predictions for the total volume fraction of mixed material f ($=2T_{A/B}/D$) and the microdomain periodicity D are presented in Figure 6. As $\phi_A^{(A/B)}(0)$ increases from 0.5, D is predicted to decrease, which coincides with a surprisingly large increase in f. Both of these functional relationships suggest that a composition gradient imposed across the middle A/B block enhances interfacial mixing and end-block solubilization. The predicted f and D in Figure 6 reflect the influence of tapering only, since both the molecular composition and weight are held constant at 0.3:0.4:0.3 A:A/B:B and 2×10^5, respectively. From the thermodynamic predictions provided here, along with the detailed morphological studies by Hashimoto et al.,[24] compositional tapering clearly constitutes an additional design parameter in the synthesis of A(A/B)B copolymers, one which may prove valuable in certain applications.[38]

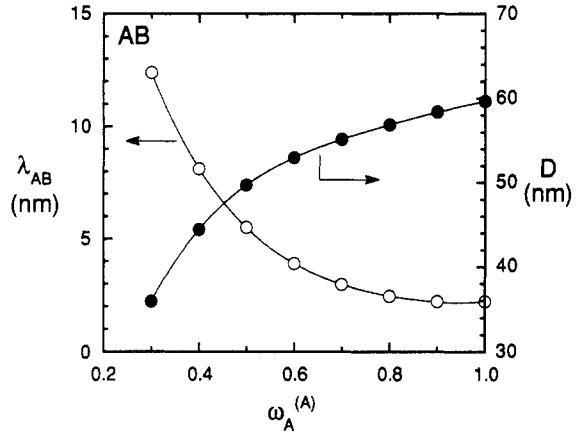

Figure 7. Predicted microstructural dimensions λ_{AB} (○) and D (●) as functions of $\omega_A^{(A)}$ for the case in which the B block of an AB copolymer is pure B ($\omega_A^{(B)} = 0.0$). As the A block becomes more mixed, the interphase thickness is predicted to increase substantially, in qualitative agreement with the narrow interphase approximation[15] (i.e., χ_{AB} decreases and λ_{AB} increases as $\omega_A^{(A)}$ decreases from unity). The microdomain periodicity (D) is observed to decrease as the A block becomes less pure, also reflecting an increase in phase mixing.

Conclusions

A model based on the confined-chain statistics originally developed[13,14] for diblock copolymers is presented to (i) identify the molecular characteristics responsible for producing a three-microphase A(A/B)B block copolymer and (ii) elucidate the relationships existing between molecular and microstructural characteristics within this regime. Boundary conditions associated with the SSL have

Table I
Molecular and Microstructural Characteristics of Some Impure AB Copolymers[a] and Model Predictions

			experimental					theoretical		
sample code	ref	diene	M (×10^{-3})	w_A	$\omega_A^{(A)}$	D^b (nm)	D^c (nm)	D (nm)	f	Δg_{min} (kJ/mol)
P3	24	butadiene[d]	119.0	0.57	0.26	47	43	42.3	0.22	−24.0
P4	24	butadiene[d]	93.0	0.50	0.20	41	36	36.3	0.25	−21.6
IS40	26	isoprene	193.0	0.40	0.50	54		50.0	0.19	−33.4

[a] These AB copolymers are of the form (S/X)S, where S refers to styrene and X to a diene. [b] Values estimated from TEM micrographs; expected error ±2 nm. [c] Values obtained from SAXS spectra; assigned error ±1 nm. [d] Physical properties of polybutadiene are ρ = 0.97 g/cm^3, δ = 8.3 H, and K = 0.086 nm.

been employed to determine the range of model applicability in terms of block and molecular composition and molecular weight. Limits to this model arise when (i) $w_{A/B}$ becomes sufficiently small (two-microphase degeneration) or large (microstructural disorder), (ii) $\omega_A^{(A/B)}$ deviates far from 0.5 (preferential end-block solubilization), and (iii) M is too small (microstructural disorder). Estimates of the molecular characteristics responsible for the onset of the WSL have also been obtained and indicate that the boundary conditions imposed here restrict this model to the SSL.

Predictions of the microstructural dimensions have also been provided, with particular emphasis on the microdomain periodicity (D) and the middle microdomain ($T_{A/B}$) as functions of these molecular parameters. It has been found that $D(w_{A/B} = 0) > D(w_{A/B} > 0)$, which reflects the increased degree of molecular mixing upon insertion of the A/B block. Both $T_{A/B}$ and the corresponding volume fraction of mixed material (f) are predicted to increase monotonically with $w_{A/B}$. If the middle A/B block is compositionally tapered, predictions provided here reveal that solubilization of both end blocks is enhanced.

Acknowledgment. J.M.Z. gratefully acknowledges the Exxon Chemical Co. for financial support. We also thank The Pennsylvania State University for computing time and Dr. I. Noda and Mr. A. Ashraf for discussions which prompted this work.

Appendix. The "Mixing-in-Domain" Effect on the Morphology of Diblock Copolymers

A key assumption employed within the text is that the middle A/B block possesses statistically random sequencing. Here, we address the issue of a diblock copolymer in which one or both blocks is random. Block copolymers of this type have been synthesized by both Hashimoto et al.[24] and Bühler and Gronski.[26] Unlike materials exhibiting the "domain-boundary-mixing" effect, copolymers of this type possess either A or B microdomain cores which remain partially phase-mixed.

The equations put forth in the text can be used to model this variation of the A(A/B)B molecular architecture with only minor modifications. The first foremost alteration to note is that, since only one unique interphase exists between the impure A and B blocks, only two parameters ($\beta_{AB} \equiv \lambda_{AB}/T_A$ and Γ) are required in the free-energy minimization. This feature also allows Δh (eqs 3, 4, and 6 in the text) to be conveniently combined and rewritten as

$$\Delta h = -v\Delta\delta_{AB}^2 \left\{\Phi_A\Phi_B - \frac{f_{AB}}{8}(4[\phi_A^{(A)} + \phi_A^{(B)}] - 3[(\phi_A^{(A)})^2 + (\phi_A^{(B)})^2] + \tau_{AB}\pi^2[\phi_A^{(A)} - \phi_A^{(B)}]^2)\right\} \quad \text{(A1)}$$

where the microdomain compositions ($\phi_A^{(A)}$ and $\phi_A^{(B)}$) are obtained from eq 5. Equation A1 is sufficiently general to account for impurity in both blocks and, in the limit of both blocks being pure, correctly reduces to the expression for an ideal diblock copolymer.[14,28,31] The entropic contribution to Δg consists of only one Δs_{AB} term (eq 7) and the two expressions in the summation of eq 8. Finally, Meier's approach to uniform core density in both microdomains is accurately described by the single relationship found in eq 10a.[13]

In Figure 7, λ_{AB} and D are provided as functions of the purity of block A ($\omega_A^{(A)}$) for the case when the B block is pure B (i.e., $\omega_A^{(B)} = 0.0$). [The corresponding ideal diblock copolymer, possessing $w_A = w_B = 0.5$ and $M = 2 \times 10^5$, is given by $\omega_A^{(A)} = 1.0$.] From Figure 7, λ_{AB} is predicted to increase, while D decreases, as the A block becomes less pure ($\omega_A^{(A)} < 1.0$). This feature indicates that the "mixing-in-domain" effect decreases the energetic preference for microphase separation, resulting in enhanced phase mixing and eventually leading to disorder in the WSL ($\Delta g_{min} \rightarrow 0$). Corresponding predictions for $\Delta g_{min}(\omega_A^{(A)})$, not provided here, support this observation.

Micrographs of impure diblock copolymers have been obtained with TEM and, along with corresponding SAXS spectra (acquired using edge radiation), clearly reveal that these materials exhibit ordered lamellar morphologies, despite relatively high levels of residual phase mixing. More recent efforts by Ashraf et al.[39] have demonstrated that copolymers in which both blocks are impure (i.e., neither $\omega_A^{(A)}$ nor $\omega_B^{(B)}$ is equal to unity) are capable of microphase-separating. Predictions of D from the present model are provided in Table I for several A(A/B) copolymers reported by Hashimoto et al.[24] and Bühler and Gronski.[26] Microdomain periodicities are estimated from TEM micrographs and SAXS data (recognizing that $D = 1/S^*$, where S^* is the peak scattering vector) and are also tabulated in Table I. A comparison of model predictions with experimental data reveals very good agreement.

Nomenclature

a	scaling exponent for $T_{A/B}(M)$
A_i	characteristic length of microdomain i (nm)
b	scaling exponent for $D(M)$
C	constants used in eq 10a,b
D	microdomain periodicity (nm)
f	total volume fraction of mixed material
f_{ij}	volume fraction of material in λ_{ij}
g	molar Gibbs free energy (kJ/mol)
h	molar enthalpy (kJ/mol)
K_i	Kuhn segment length of monomer i (nm)
L_i	microdomain core of block i (nm)
m	number of characteristic regions in the system
M	total molecular weight
M^*	renormalized molecular weight
N	number of monomers per molecule
R	gas constant (1.9872 cal/mol·K)
$\langle r_i^2\rangle^{1/2}$	perturbed rms end-to-end distance of block i (nm)

$\langle r_i^2\rangle_0^{1/2}$	unperturbed rms end-to-end distance of block i (nm)
s	molar entropy (kJ/mol·K)
S^*	peak scattering vector (nm^{-1})
t	Debye interaction parameter (nm)
T	absolute temperature (K)
T_g	glass transition temperature (K)
T_i	microdomain region including core and interphases (nm)
v	total molar volume (cm^3/mol)
v_i	molar volume of block i (cm^3/mol)
w_i	weight fraction of block i
w^*_i	renormalized weight fraction of block i
W_i	bulk weight fraction of monomer i

Greek Letters

α_i	expansion coefficient of block i
β_{ij}	minimization parameter corresponding to λ_{ij}
χ_{ij}	Flory–Huggins interaction parameter between monomers i and j
δ_i	solubility parameter of monomer i (H)
Φ_i	volume fraction of block i
$\phi_i^{(j)}$	volume fraction of monomer i in block j
$\phi_i^{(j)}(x^*)$	volume fraction of monomer i in block j at position x^*
Γ	minimization parameter defined by eq 12
λ_{ij}	thickness of the ij interphase (nm)
ρ_i	mass density of block i (g/cm^3)
σ_i	dimensionless variable in eq 8
τ_{ij}	interaction parameter normalized with respect to λ_{ij}
$\omega_i^{(j)}$	weight fraction of monomer i in block j
ξ_{ij}	ratio of physical properties between blocks i and j

References and Notes

(1) Stoeppelmann, G.; Gronski, W.; Blume, A. *Polymer* **1990**, *31*, 1838.
(2) Noda, I.; Smith, S. D.; Dowrey, A. E.; Grothaus, J. T.; Marcott, C. *Mater. Res. Soc. Symp. Proc.* **1990**, *171*, 117.
(3) Gronski, W.; Stoeppelmann, G.; Blume, A. *Polym. Prepr. (Am. Chem. Soc., Div. Polym. Chem.)* **1988**, *29*, 46.
(4) Roe, R.-J.; Fishkis, M.; Chang, J. C. *Macromolecules* **1981**, *14*, 1091.
(5) Hashimoto, T.; Shibayama, M.; Kawai, H. *Macromolecules* **1980**, *13*, 1237.
(6) Hashimoto, T.; Fujimura, M.; Kawai, H. *Macromolecules* **1980**, *13*, 1660.
(7) Richards, R. W.; Mullin, J. T. *Mater. Res. Soc. Symp. Proc.* **1987**, *79*, 299.
(8) Richards, R. W.; Thomason, J. L. *Polymer* **1983**, *24*, 1089.
(9) Bates, F. S.; Berney, C. V.; Cohen, R. E. *Macromolecules* **1983**, *16*, 1101.
(10) Satija, S. K.; Majkrzak, C. F.; Anastasiadis, S. H.; Russell, T. P. *Mater. Res. Soc. Symp. Proc.* **1990**, *166*, 139.
(11) Anastasiadis, S. H.; Russell, T. P.; Satija, S. K.; Majkrzak, C. F. *J. Chem. Phys.* **1990**, *92*, 5677.
(12) Anastasiadis, S. H.; Russell, T. P.; Satija, S. K.; Majkrzak, C. F. *Phys. Rev. Lett.* **1989**, *62*, 1852.
(13) Meier, D. J. In *Block and Graft Copolymers*; Burke, J. J., Weiss, V., Eds.; Syracuse University Press: Syracuse, NY, 1973; Chapter 6. Meier, D. J. *J. Polym. Sci., Part C* **1969**, *26*, 81; *Polym. Prepr. (Am. Chem. Soc., Div. Polym. Chem.)* **1974**, *15*, 171. Meier, D. J. In *Thermoplastic Elastomers: A Comprehensive Review*; Legge, N. R., Holden, G., Schroeder, H. E., Eds.; Hanser Publishers: New York, 1987; Chapter 12.
(14) Leary, D. F.; Williams, M. C. *J. Polym. Sci., Polym. Phys. Ed.* **1973**, *11*, 345; **1974**, *12*, 265. Henderson, C. P.; Williams, M. C. *J. Polym. Sci., Polym. Phys. Ed.* **1985**, *23*, 1001.
(15) Helfand, E.; Wassermann, Z. R. *Macromolecules* **1976**, *9*, 879; **1978**, *11*, 960; **1980**, *13*, 994. Helfand, E. In *Recent Advances in Polymer Blends, Grafts and Blocks*; Sperling, L. H., Ed.; Plenum Press: New York, 1974. Helfand, E. *Macromolecules* **1975**, *8*, 552. Helfand, E. In *Developments in Block Copolymers*; Goodman, I., Ed.; Applied Science: London, 1982; Vol. I.
(16) Almdal, K.; Rosedale, J. H.; Bates, F. S.; Wignall, G. D.; Fredrickson, G. H. *Phys. Rev. Lett.* **1990**, *65*, 1112.
(17) Almdal, K.; Rosedale, J. H.; Bates, F. S. *Macromolecules* **1990**, *23*, 4336.
(18) Koberstein, J. T.; Russell, T. P.; Walsh, D. J.; Pottick, L. *Macromolecules* **1990**, *23*, 877.
(19) Bates, F. S.; Bair, H. E.; Hartney, M. A. *Macromolecules* **1984**, *17*, 1987.
(20) Bates, F. S. *Macromolecules* **1985**, *18*, 525.
(21) Han, C. D.; Kim, J. *J. Polym. Sci., Polym. Phys. Ed.* **1987**, *25*, 1741.
(22) Leibler, L. *Macromolecules* **1980**, *13*, 1602.
(23) Rounds, N. A. Ph.D. Dissertation, University of Akron, Akron, OH, 1970.
(24) Hashimoto, T.; Tsukahara, Y.; Tachi, K.; Kawai, H. *Macromolecules* **1983**, *16*, 648.
(25) Annighöfer, F.; Gronski, W. *Colloid Polym. Sci.* **1983**, *261*, 15; *Makromol. Chem.* **1984**, *185*, 2213.
(26) Bühler, F.; Gronski, W. *Makromol. Chem.* **1986**, *187*, 2019; **1987**, *188*, 2995; **1988**, *189*, 1087.
(27) Spontak, R. J.; Williams, M. C. *J. Macromol. Sci., Phys.* **1989**, *B28*, 1.
(28) Spontak, R. J.; Zielinski, J. M. *Macromolecules* **1992**, *25*, 663.
(29) Flory, P. J. *Principles of Polymer Chemistry*; Cornell University Press: Ithaca, NY, 1953; p 549.
(30) Prausnitz, J. M.; Lichtenthaler, R. N.; de Azevedo, E. G. *Molecular Thermodynamics of Fluid-Phase Equilibria*; Prentice-Hall: Englewood Cliffs, NJ, 1986; p 290.
(31) Recent theoretical results by G. H. Fredrickson and S. T. Milner (*Phys. Rev. Lett.* **1991**, *67*, 835) indicate that random copolymer melts may become mesomorphic under certain conditions of molar composition, chemical dissimilarity, molecular weight, and monomer sequencing. Here, we assume that the random A/B middle block remains microscopically homogeneous even after microphase separation.
(32) Experimental evidence suggests that the interphase composition profile is asymmetric. For detailed discussions on this subject, see, in addition to ref 1: Henderson, C. P.; Williams, M. C. *Polymer* **1985**, *26*, 2021. Spontak, R. J.; Williams, M. C.; Agard, D. A. *Macromolecules* **1988**, *21*, 1377.
(33) Spontak, R. J.; Smith, S. D.; Ashraf, A., work in progress.
(34) Tsukahara, Y.; Nakamura, N.; Hashimoto, T.; Kawai, H.; Nagaya, T.; Sugimura, Y.; Tsuge, S. *Polym. J.* **1980**, *12*, 455. Hashimoto, T.; Tsukahara, Y.; Kawai, H. *Polym. J.* **1983**, *15*, 699.
(35) Guo, M.; Yu, T.; Xue, Z. *Makromol. Chem., Rapid Commun.* **1987**, *8*, 601.
(36) Keul, H.; Höcker, H.; Leitz, E.; Ott, K.-H.; Morbitzer, L. *Makromol. Chem.* **1988**, *189*, 2303.
(37) Matsushita, Y.; Mori, K.; Saguchi, R.; Nakao, Y.; Noda, I.; Nagasawa, M. *Macromolecules* **1990**, *23*, 4313.
(38) Fayt, R.; Teyssié, Ph. *Polym. Eng. Sci.* **1990**, *30*, 937.
(39) Ashraf, A.; Smith, S. D.; Clarson, S. J., presented at the 24th Central Regional ACS Meeting, May 1992.